Development and Experimental Validation of a DESRAD Cooling Model

M. Swami **A. Rudd** **P. Fairey**

ABSTRACT

This paper presents an analytical model with experimental validation of the desiccant-enhanced nocturnal radiation (DESRAD) cooling and dehumidification concept. This concept integrates the moisture-exchanging capacity of a roof plenum desiccant system with radiative cooling potential of the night sky and the thermal and moisture capacity of building materials to provide a high-efficiency, daily cycle cooling and dehumidification system for buildings. The model accounts for the interaction of the building and the DESRAD system by coupling a combined heat and mass transfer model for the building and a pseudo steady-state desiccant model for the DESRAD system. Modeling results are given for Atlanta, GA. Results show summer day electrical cooling savings of 67%. Peak electrical demands over a five-hour period from noon to 5 p.m. were also reduced by 46%. Comparison of the model with experimental data is favorable except for lower bed utilizations than predicted. Additional experiments are being conducted to provide a better understanding of this finding.

INTRODUCTION

In the hot humid climates of the southeastern U.S., the cooling potential of traditional passive cooling alternatives is weak. Consistently high dew- point temperatures limit diurnal temperature swings, nocturnal radiation, and evaporative cooling potential, and high ground temperatures limit earth coupling. More importantly, none of these traditional cooling strategies provides any dehumidification. It is essential that cooling strategies be capable of removing both latent and sensible loads in hot humid climates. The desiccant-enhanced nocturnal radiation (DESRAD) concept, proposed by Fairey et al. (1985), offers this potential. A preliminary analytical study of the desiccant bed (Fairey et al. 1986) showed the concept to be viable but did not directly include building interactions. The present study integrates the house and DESRAD system.

DESRAD -- Principle of Operation

The DESRAD cooling and dehumidification concept is a building integrated concept that utilizes (1) the moisture and thermal capacity of household materials to provide storage during the day, (2) a roof integrated desiccant bed to remove moisture from the house during nighttime, (3) the night sky potential to provide sensible cooling, and (4) the daytime solar and ambient potentials to regenerate the bed. This solar concept is a novel way of reducing cooling and dehumidification energy consumption in buildings.

The DESRAD system consists of a metallic roof with an integral duct containing a bed of desiccant across the airflow path. The upper surface of the duct is exposed to the ambient, while

Muthusamy Swami is research engineer, Florida Solar Energy Center; Armin Rudd is research engineer, Florida Solar Energy Center; Philip Fairey is program director, Florida Solar Energy Center, Cape Canaveral, FL.

the bottom surface is well insulated and would typically be exposed to the attic air. Air can be channeled through the system either from the house it serves or from ambient, depending on the mode of operation desired.

The basic operating modes of the concept -- nighttime adsorption and daytime desorption or regeneration -- are shown in Figure 1. At the beginning of the night, room air is circulated to the roof where it is dried by the desiccant bed. The heat of sorption warms the roof, giving it a greater sensible cooling potential with respect to ambient. The remainder of the duct path serves to post-cool the dehumidified air. The outlet air is over-dried and has the potential for further sensible cooling. An evaporative cooler is used to raise the humidity level to a desired value and further cool the air before returning it to the room. Consequently, the temperature and humidity levels in the room fall, leading the building envelope to release moisture and heat.

During daytime, the house is decoupled from the roof plenum system, relying on the internal thermal mass and moisture capacitance to carry the cooling and dehumidification loads through the day. The desiccant system is vented with ambient air that is heated by the sun-absorbing metal roof. The hot air, combined with the radiation exchange between the metal roof and desiccant bed, serves to regenerate the bed. Over the complete cycle, the DESRAD system provides both sensible and latent cooling.

The advantages of the DESRAD system include:

1. It can provide both sensible and latent cooling.
2. It takes advantage of the night sky as a heat sink.
3. It takes advantage of the moisture capacity of building materials and furnishings.
4. It uses desiccant bed geometries with low pressure drops.
5. It uses solar potentials to regenerate the bed.

The disadvantages include:

1. Air is used as the working fluid; therefore, parasitic power is not negligible.
2. Backup system is from a conventional air-conditioning system. The desiccant bed cannot be economically regenerated using an auxiliary heat source because losses to the ambient are far too great.

ANALYTICAL APPROACH

Combined heat and mass transport in the house as well as the desiccant bed are simulated. Moisture transport at the wall surfaces of the house are simulated using the Effective Moisture Penetration Depth (EMPD) concept, a simplified, lumped approach (Kerestecioglu et al. 1988). A modified version of the pseudo steady-state desiccant bed model (Barlow 1982; Collier 1988) is used for the roof desiccant system.

House Model

For convenience, the building is divided into two domains with boundaries as shown in Figure 2.

The governing balance equations for a given zone, i, may be written as:

Energy Balance:

$$(\rho_a V C_p)_i \, dTr_i/d\tau = Qwal\text{-}s_i + \sum_{j=1}^{nss} Qss\text{-}s_{i,j} \quad \text{in } \Omega_a \tag{1}$$

Moisture Balance:

$$(\rho_a V)_i \, dWr_i/d\tau = Qwal\text{-}l_i + \sum_{j=1}^{nss} Qss\text{-}l_{i,j} \quad \text{in } \Omega_a \tag{2}$$

where $Qss\text{-}s_{i,j}$ and $Qss\text{-}l_{i,j}$ are the additional source and sink terms acting on the air domain. These terms are handled routinely. Tables 1 and 2 summarize each term.

In Equations 1 and 2, $Qwal\text{-}s_i$ and $Qwal\text{-}l_i$ are the terms containing the unknowns (other than Tr and Wr) representing the energy and moisture exchanges between the room air and envelope.

They are given by:

$$Qwal\text{-}s_i = \sum_{k=1}^{nos} h_{Ti,k} A_{i,k} \, (T^*_{i,k} - Tr_i) \text{ on } \Gamma_a$$

and

$$Qwal\text{-}l_i = \sum_{k=1}^{nos} h_{Mi,k} A_{i,k} \, (W^*_{i,k} - Wr_i) \text{ on } \Gamma_a$$

The additional surface unknowns, surface temperature (T^*) and surface humidity ratio (W^*), require that two additional equations be specified in order to obtain closure.

The energy equation for the envelope contains the surface temperature (T^*) and is given by the conduction equation:

$$(\rho C_p) \, \partial T/\partial \tau = \nabla.(k \nabla T) \quad \text{in} \quad \Omega_e \tag{3}$$

with the boundary condition:

$$-k \nabla T = \begin{cases} -q''_T + h_T(T^*-T_\alpha) + \lambda h_M(W^*-W_\alpha) \text{ on } \Gamma_e \\ -q''_T + h_T(T^*-T_r) + \lambda h_M(W^*-W_r) \text{ on } \Gamma_a \end{cases}$$

The other equation required for closure is obtained from the moisture transfer equation at the envelope surface. The lumped mass transfer equation for the i-th solid domain is given by:

$$(A \rho_b \delta_M)_i \frac{dU_i}{d\tau} = \begin{cases} h_{M,i} A_i \, (W_\alpha - W^*_i) & \text{in } \Omega_e \text{ on } \Gamma_e \\ h_{M,i} A_i \, (W_r - W^*_i) & \text{in } \Omega_e \text{ on } \Gamma_a \end{cases} \tag{4}$$

where δ_M is the thickness of material that actively participates in the moisture interaction and W^* represents the surface air humidity ratio as derived from the moisture isotherm using the moisture content (U) and temperature (T^*) of the surface. A detailed account of this concept and its applicability can be found in Keresteciogłu et al. (1988, 1989).

The EMPD concept assumes that a thin layer (δ_M) close to the wall surface behaves dynamically and exchanges moisture with the air domain when exposed to cyclic air moisture pulses. For short periods where the cyclic integral of the total moisture adsorption and desorption is near zero (i.e., there is no net moisture storage), the EMPD concept has been shown to be a reasonable approximation of reality (Keresteciogłu et al. 1989). In other words, the following constraint must be met:

$$\int_{\tau_1}^{\tau_2} \frac{dU}{d\tau} \, d\tau \simeq 0 \tag{5}$$

where, τ_2-τ_1 denotes the finite time interval over which the equation holds. The EMPD model assumes no spatial distribution of moisture content across the thickness (L) of the solid; rather, a thin layer (δ_M) of uniform moisture content (U) is assumed to represent the total moisture content of the solid. This may be mathematically stated as:

$$\int_0^L U(x) \, dx = U \, \delta_M \qquad \text{for all } \tau \tag{6}$$

For most building materials, the equilibrium moisture sorption isotherm can be defined by the following general equation (Keresteciogłu et al. 1988):

$$U = a \, \phi^b + c \, \phi^d \tag{7}$$

where

$$\phi \simeq W^*/W^*_{sat} \tag{8}$$

and

$$W^*_{sat} = \frac{1}{R_v \rho_a T^*} \exp\left(23.7093 - \frac{4111}{T^* - 35.45}\right) \tag{9}$$

Given that $U=U(W^*,T^*)$, the moisture content may be differentiated with respect to time in the following manner:

$$\frac{dU}{d\tau} = \frac{\partial U}{\partial W^*}\frac{dW^*}{d\tau} + \frac{\partial U}{\partial T^*}\frac{dT^*}{d\tau} = A_T \frac{dW^*}{d\tau} - B_\rho \frac{dT^*}{d\tau} \tag{10}$$

where A_T and B_ρ are the isothermal moisture capacity and thermo-gradient coefficient, respectively. From Equations 7, 8, and 9, they can be expressed as:

$$A_T = (ab\,\phi^b + cd\,\phi^d)/W^* \tag{11}$$

$$B_\rho = -\left[(1/T^*) - \frac{4111}{(T^* - 35.45)^2}\right](ab\,\phi^b + cd\,\phi^d) \tag{12}$$

Using Equations 10, 11, and 12 and substituting into Equation 5, one obtains the final equation needed for closure.

$$(A\rho_b\delta_M A_T)_i\, dW^*_i/d\tau = h_{M,i}A_i\,(W_\alpha - W^*_i) + (A\rho_b\delta_M B_\rho)_i \frac{dT^*_i}{\partial\tau} \text{ on } \Gamma_e$$

or

$$= h_{M,i}A_i\,(W_r - W^*_i) + (A\rho_b\delta_M B_\rho)_i \frac{dT^*_i}{\partial\tau} \text{ on } \Gamma_a \tag{13}$$

Equations 1, 2, 3, and 13 are the complete set of equations required to solve for the heat and moisture transport in the building. A more detailed account of the numerical solution procedure can be found in Keresteciogl u et al. (1988).

DESRAD Model Schematic

The roof desiccant system can be considered as an air duct divided into sections by desiccant beds as shown in Figure 3. The roof duct is exposed to ambient at the top and to the attic air at the bottom. The airstream flows through the duct system, and moisture adsorption and desorption take place during nighttime and daytime, respectively.

Consider the duct system model as having a number of air sections separated by desiccant beds, as shown in Figure 3. T_{in} and W_{in} are the entering air temperature and humidity ratio, respectively, and T_{out} and W_{out} are the temperature and humidity ratio of the air leaving the system. Radiant heat transfer takes place between two desiccant bed surfaces facing each other and between desiccant bed surfaces and inside top and bottom duct walls as indicated in the figure. Thus, a particular desiccant bed is coupled to the previous and next air duct sections and desiccant beds by radiant heat transfer. Thus the problem is nonlinear and requires an iterative solution technique.

Each air section can be solved separately. For a particular air section, its inlet conditions are the outlet conditions of the desiccant section immediately preceding it. During the adsorption mode, the inlet conditions (T_{in}, W_{in}) are those of the room air, and during the desorption mode, the inlet conditions are those of the ambient air.

Similarly, each desiccant bed section can be solved independently. For a particular desiccant section, its inlet conditions are the outlet conditions of the air section immediately upstream.

Thus, each desiccant bed and each air section is solved independently, one by one, until an overall convergence criterion is satisfied.

Duct Model

Each air section is discretized by the nodes as shown in Figure 4a. Each division of the air section contains three nodes, two nodes representing the duct walls and one representing the air in the duct. It is assumed that the metallic plates constituting the duct walls are highly conductive and massless. Figure 4b shows the resistance capacitance network and the modes of heat transfer for a typical air segment.

The analysis of the duct is through a simple energy balance model. Note that dividing the duct into N sections results in 3N nodes and 2N + 2 radiant surfaces (2N in the duct and two additional surfaces for the desiccant bed surfaces participating in radiation). In the air duct model, the meaning assigned to the subscripts are as follows:

i = represents the top plate
j = represents the air
k = represents the bottom plate
α = represents ambient
o = represents outside surface
b = represents bed surface

The governing equation for a node, i, representing the top metallic duct surface is given by:

$$\alpha_i A_i I_i - h_{Ti\alpha} A_i (T_i - T_\alpha) - \sigma \epsilon_{io} A_i F_{i,sky} (T_i^4 - T_{sky}^4) - h_{Tij} A_i (T_i - T_j)$$

$$- \sigma \sum_{l=1}^{nor} A_i f_{il} (T_i^4 - T_l^4) - \sigma \sum_{l=1}^{nob} A_i f_{il} (T_i^4 - T_{bl}^4) = 0 \qquad (14)$$

where the terms are:

1st term:: = energy due to solar radiation incident on the outside surface of the duct
2nd term:: = represents convection to ambient air
3rd term:: = radiant energy exchange with sky
4th term:: = convection to the airstream in the duct
5th term:: = radiant exchange between node i and all other nodes on the duct surfaces
6th term:: = radiant exchange between node i and any desiccant surface it sees

The energy balance for the bottom duct surface will be qualitatively the same as Equation 14.

For the air-node, j, the energy balance equation is given by:

$$h_{Tij} A_i (T_i - T_j) + h_{Tk} A_k (T_k - T_j)$$

$$+ m^o C_{Pa} ((T_j)_{in} - (T_j)_{out}) + m_j C_{pa} \frac{dT_j}{d\tau} = 0 \qquad (15)$$

where

1st term:: = heat transfer to the top node by convection
2nd term:: = heat transfer to the bottom node by convection
3rd term:: = net energy transfer due to inflow and outflow
4th term:: = change in energy of the node

T_j, $(T_j)_{in}$, and $(T_j)_{out}$ can be related through an effectiveness,

$$\eta = \frac{T_j - (T_j)_{in}}{(T_j)_{out} - (T_j)_{in}}$$

We assumed an effectiveness, η=1.0

A system of N algebraic equations will result when the air duct is discretized by N nodes. This system of equations is solved to obtain the temperature of each node.

Desiccant Bed Model

The desiccant bed is modeled using Barlow's (1982) algorithm as modified by Collier (1988). The model has been further modified by Swami et al. (1989) to incorporate intersurface radiation.

Figure 5a shows a schematic of one desiccant bed in the system. Each desiccant bed is divided into N number of isothermal sections. The first and final sections of the desiccant bed are coupled to the top and bottom plates of the adjacent air sections and adjacent desiccant beds through radiation.

In Figure 5b, the conditions entering and leaving the desiccant subsections are T_{a1}, W_{a1} and T_{a2}, W_{a2}, respectively. T_{b1}, X_{b1} and T_{b2}, X_{b2} are the desiccant bed section's temperature and moisture content at the beginning and end of the time step, respectively. Each desiccant bed subsection is solved separately, and the outlet temperature and humidity ratio of each desiccant bed subsection serve as the inlet temperature and humidity ratio for the next previous desiccant bed subsection.

This model first calculates the moisture content of the air and desiccant bed section, keeping the temperature constant. The outlet air humidity ratio and moisture content of the desiccant bed section are calculated based on a moisture balance. Next, an energy balance is performed considering the heat of sorption, and an intermediate bed temperature is obtained. The intermediate bed temperature and the inlet air temperature are then used with the intersurface radiation algorithm in the heat transfer calculations to determine the process air and desiccant bed temperatures.

Intersurface radiation is only considered for the first and last desiccant bed sections in performing these calculations. Radiation makes the problem nonlinear, and the Newton-Raphson iterative method is used to achieve solution. The calculations are performed for each desiccant bed section, and the resulting bed outlet conditions are used as the inlet conditions for the next air section.

Mass Transfer

The effectiveness equation for a parallel flow energy exchanger is used for mass transfer calculations. The assumptions for this calculation are that the air is in equilibrium at the desiccant bed surface and all temperatures are constant. The steps to obtain the mass transfer are as follows:

1. Mass of water sorbed, m_{sorb}

$$m_{sorb} = E_M \, Cmin \, (P_{w1} - P_{ve1}) \tag{17}$$

where

E_M = parallel flow exchanger effectiveness

$$= \frac{1 - e^{-NTU\ (1+Cmin/Cmax)}}{1 + Cmin/Cmax} \tag{18}$$

and

$$NTU = h_m A_s/(R_w \, T_{a1} \, Cmin)$$

where Cmin and Cmax are the minimum and maximum moisture capacities, respectively, between the air and desiccant sections

2. Outlet humidity ratio, W_{a2}

$$W_{a2} = W_{a1} - m_{sorb}/m_a \tag{19}$$

3. New bed moisture content, X_{b2}

$$X_{b2} = (X_{b1} \, m_b + m_{sorb}/m_a) \tag{20}$$

Energy Balance

After the mass transfer is calculated, an energy balance is performed to calculate the intermediate bed section temperature due to the energy exchange. The energy balance between the airstream and bed section can be written as,

$$m_a(h_a^* - h_{a1}) + m_b[(C_b + X_{b2}C_w)T_b^{\#} - (C_b + X_{b1}C_w)T_{b1}] - m_b H_{WET}$$

$$+ \sigma \sum_{1=1}^{nor} f_{i1} (T_{b2}^4 - T_1^4) + \sigma \sum_{1=1}^{nob} f_{i1} (T_{b2}^4 - T_{b1}^4) = 0 \qquad (21)$$

where

1^{st} term:: = energy exchange for air
2^{nd} term:: = energy exchange for bed
3^{rd} term:: = heat of wetting
4^{th} term:: = radiant heat exchange between bed section surface and duct wall surface
5^{th} term:: = radiant heat exchange between bed section surface and previous and/or next bed section surface

and

$$h_a^* = h^*(T_{a1},W_{a2}), \qquad h_{a1} = h(T_{a1},W_{a1})$$

The above equation is written in terms of an unknown intermediate bed temperature, $T_b^{\#}$.

Heat Transfer Calculation

After determining the intermediate temperature for the bed section, the final bed section and air temperature are calculated using the parallel flow heat exchanger equation. The heat transfer, Q, is given by,

$$Q = E_T \, Cmin \, (T_b^{\#} - T_{a1}) \, d\tau \qquad (22)$$

where E_T is the effectiveness of the heat exchanger, derived as:

$$E_T = \frac{1 - e^{-NTU(1+Cmin/Cmax)}}{(1+Cmin/Cmax)}$$

and

$$NTU = h_T A_s / Cmin$$

where Cmin and Cmax are the minimum and maximum between the air thermal capacity ($m_a \, dh/d\tau$) and bed thermal capacity ($C_b + m_b X_b C_w$). Based on this heat transfer, (Q), T_{a2} and T_{b2} are determined as follows,

$$T_{a2} = T_{a1} + Q/(m_a C_{pa}) \qquad (23)$$

$$T_{b2} = T_b^{\#} + Q/[m_b(C_b + X_{b2}C_w)] \qquad (24)$$

Equations 23 and 24 are solved iteratively with Equation 21.

Validation and comparison of the house model with experimental data are given by Keresteciogl u et al. (1989). Validation of the pseudo-steady-state desiccant model and comparison with experimental data are given by Barlow (1982). Collier (1988) compared the results of his pseudo-steady-state model with McClain-Cross' (1974) algorithm and obtained good agreement. As a debug procedure, the code discussed here was run using Barlow's (1982) inputs.

SYSTEM AND SIMULATION PARAMETERS

Base House

Residence type:
Single-story slab on grade with garage

Aspect ratio 1:1.6, major axis east-west

Window glass:
Gross area: 10% of gross floor area
Area: North and south 13 m^2.
Shading coefficient: south 0.87, all other 0.2

Floor:
Construction: 0.102 m (4 in.) structural slab on grade,
Area: 139 m^2

Walls:
Construction: (from interior) 0.0127 m (1/2 in.) gypsum on 4 mil vapor barrier, R-11 batt infill on 0.01 m (7/16 in.) masonite exterior siding
Solar absorptance: 0.75
Internal partition: 0.025 m (1 in.) gypsum, area 104 m^2
EMPD for gypsum 0.003 m
Specific heat increased 15 times to simulate wallboard for DESRAD house

Ceiling:
Construction: 0.0127 m (1/2 in.) gypsum with R-19 insulation
Area: 139 m^2

Roof:
The attic was not specifically modeled. It was assumed that the underside of the roof plenum was well ventilated so that convection from the ceiling insulation was to air at ambient conditions.

Loads:
Scheduled infiltration totalling 12 AC/day
Scheduled sensible generation totalling 47 MJ/day
Scheduled latent generation totalling 10.9 kg/day

Machine:
Typical two-ton air-conditioning unit
Setpoint: 25.56°C (78°F)

DESRAD

Duct:
Length 10.5 m, width 14 m, height 0.15 m

Desiccant: Silica gel
Total volume: 0.12 m^3 per unit (m) width, thickness 0.0125 m, two beds spanning 4.75 m across duct

Density of bed	720 kg/m_3.	(Barlow 1982)
Specific heat, C_p	921 J/kg^0K	(Barlow 1982)
Lewis number	3.0	(Barlow 1982)
Particle diameter	0.00193 m	(Barlow 1982)
Total surface area	1335.0 m^2/m^3	(Barlow 1982)
Max moisture content	0.36 kg/kg	(from manufacturer)
Isotherm	nonlinear curve fit	(data from manufacturer)
DHSHV	0.3	(Jurinak 1982)
Rate factor	5.0	(Jurinak 1982)

Other:
Evaporative cooler setpoint: 58% RH
Adsorption/desorption control:
Automatic (adsorption mode if $h_{room} > h_{des}$
Desorption mode if $w_{des} > w_{room}$
Otherwise idle mode (flow reduced by a 10th)
Airflow: 0.085 m^3/s (180 cfm) per unit width of duct

RESULTS

Single-day runs were made for Atlanta for typical summer conditions with weather data extracted from TMY weather tapes. The base for comparison was the frame house with no desiccant system. The DESRAD house had both a desiccant system and high-capacity (PCM impregnated) gypsum wallboard.

The single-day simulation was actually a 10-day run using the same daily ambient data. This ensured that the initial starting condition of the house as well as the desiccant system did not affect the outcome of the calculated loads.

Figure 6 compares the cooling load requirements (total, sensible, and latent) of the base house and DESRAD house for Atlanta weather. During nighttime and early morning hours when the DESRAD system is in the adsorption cycle, the load on the air conditioner is zero. During other times, the loads on the DESRAD house are much lower than the base house. The savings in total, sensible, and latent loads for the DESRAD house were 67%, 68%, and 68%, respectively. Peak load reduction from noon to 5 p.m. was 46%.

Figure 7 compares the indoor conditions for the two cases in Atlanta. Nighttime temperatures in the DESRAD house are 1 to 2 degrees lower than in the base house, providing extra cold storage. Nighttime relative humidities in the DESRAD house are up to 10% lower than in the base house, providing extra moisture storage capability. The afternoon and evening relative humidities are about 6% higher in the DESRAD house to allow moisture storage in the building materials and furnishings. However, the peak relative humidity in the DESRAD house is nearly 10% less than in the base house.

The wall fluxes, both sensible and latent, show sharp reversals when the desiccant system is added to the house. Nighttime sensible fluxes from the walls are substantially increased, while daytime sensible wall fluxes are substantially decreased. For the base house, the walls adsorb moisture during nighttime and release moisture during daytime. This tendency is reversed in the DESRAD house with desorption taking place during late evening hours. The reversals created by the DESRAD system provide for the use of building materials as thermal and moisture storage. The water adsorbed for the DESRAD system over the course of the Atlanta summer day was 93 kg. Utilization factor (β) is a dimensionless parameter used to analyze the desiccant bed efficiency. Bed utilizations of above 85% were achieved with this desiccant configuration.

COMPARISON WITH EXPERIMENTAL DATA

Diurnal Test Facility

Currently, experimental research is being conducted on the DESRAD concept using the Diurnal Test Facility (DTF). The DTF is a state-of-the-art, computer-automated roof testing facility and was designed to study roof integrated cooling strategies. The effects of solar heating potential and nocturnal cooling potential are simulated in a controlled indoor environment. Figure 8 shows a picture of the test facility. Air delivered to the test section is controlled to close tolerances. The basic layout of the air delivery apparatus is illustrated in Figure 9. Steady-state conditions, step changes, functional changes, or real weather conditions can be simulated. Extensive instrumentation provides measurements of temperature, humidity, pressure, and airflow rate. Primary experimental data are taken inside the ducted test bed. Measurements taken at the inlet and outlet of the test bed determine the amount of heat and mass transfer through the system. Figure 10 shows a cross sectional view of the test bed with its top and bottom plates separated by aluminum channels. The facility is completely computer controlled. The control software, employing a self-tuning proportional-integral control methodology, was developed in house.

Sample Results

Tests on the dual-bed configuration have been completed. The data shown in Figure 11 were produced by the DTF and compared to the predictions made by the analytical model. The figure shows how the dry-bulb temperature of the supply air was held constant while the dew-point temperature was changed every eight hours to give a 37% step change in relative humidity. For the given inlet conditions, the model's prediction of the central and outlet dew-point and dry-bulb temperatures are plotted against the experimental data in Figure 12.

The major problem that we have encountered thus far seems to be a partial utilization of the desiccant in the bed. For the best model prediction of experimental data, shown in Figure 12, the amount of desiccant available for moisture transport was reduced by 65%. The associated effect reduces the expected DESRAD energy savings by 15%. We are currently conducting more tests, both with the DTF and in an environmental chamber, to isolate the source of this lower bed utilization, which we suspect to be due either to fluid dynamics or hysteresis in the isotherm.

Tests in the environmental chamber will investigate the problem from a material viewpoint. Several grades of silica gel will be tested at the same time, each with a different particle size, in order to investigate a possible problem with solid side resistance to moisture movement into and out of the desiccant particle. Further testing with the DTF is designed to isolate possible problems with fluid dynamics, which may cause portions of the sloping desiccant beds to be bypassed.

Result Uncertainty

An analysis of the measurement uncertainty for the DTF data has been conducted according to the ANSI/ASME standard for measurement uncertainty, (ANSI/ASME 1985). Table 3 gives the input parameters for the analysis. A summary of the uncertainty for the final results is given in Table 4. Uncertainties are shown for the 95% and 99% coverage methods of calculation.

CONCLUSION

A building integrated DESRAD system has be studied both analytically and experimentally. The results indicate that DESRAD is a promising solar cooling alternative with significant potential savings in hot, humid climates. However, before concrete recommendations can be made, more research is needed. Current experimental efforts show reduced bed utilizations of up to 65%. Testing to isolate the source of the problem is underway using the Diurnal Test Facility and an environmental chamber.

ACKNOWLEDGEMENT

The authors gratefully acknowledge the U.S. Department of Energy (DOE) for funding this research. We are grateful to Mr. David Pellish, Mr. Robert Hughey and Mike Lopez of DOE for their continued encouragement of this work. We would also like to thank Dr. Kirk Collier of FSEC for his insight and assistance throughout the course of the model analysis.

NOMENCLATURE

A = Area [m^2]
A_s = Surface area of desiccant [m^2/m^3]
A_T = Isothermal moisture capacity
B_ρ = Thermo-gradient coefficient [kg/kg-K]
C = Capacity (thermal or moisture)
C_p = Specific heat [J/kg.K]
C_w = Heat capacity of water [J/kg.K]
DHSHV = Excess fraction of heat of adsorption
E_M = Effectiveness for mass transfer
E_T = Effectiveness for heat transfer
EI = Infiltration [l/s]
EM = Internal air flow from zone [l/s]
EV = Ventilation air flow from zone [l/s]
F = View factor
fc = Convective fraction of heat from lights
h = Enthalpy [J/kg]
h_M = Convective mass transfer coefficient [kg/m^2-s]
h_T = Convective heat transfer coefficient [W/m^2-K]
I = Incident solar insolation [W/m^2]
II = Exfiltration [l/s]
IM = Internal air flow to zone [l/s]
IV = Ventilation air flow to zone [l/s]
k = Thermal conductivity [W/m-K]
L = Length [m]

m = Mass [kg]
m^o = Mass flow rate of air [kg/s]
nob = Number of beds exposed to radiation
nor = Number of radiating surfaces
nos = Number of heat transfer surfaces
noz = Number of zones
Np = Number of people
nss = Number of source and sink terms
P = Pressure [N/m^2]
P_w = Partial pressure of water vapor in air [N/m^2]
P_v = Equilibrium vapor pressure in desiccant [N/m^2]
q''_M = Imposed moisture flux [kg/m^2-s]
q''_T = Imposed heat flux [W/m^2]
R_v = Ideal gas constant [461.52 J/kg-K]
Re = Radiative fraction of heat from equipment
Rp = Radiative fraction of heat from people
T = Temperature [K]
U = Moisture content [kg/kg] of building material
Ue = Equipment utilization coefficient
Ul = Lighting utilization coefficient
V = Volume [m^3]
W = Humidity ratio [kg/kg]
We-l = Latent heat gain from equipment [W]
We-s = Sensible heat gain from equipment [W]
Wl = Sensible heat gain from light [W]
Wp-l = Latent heat gain from people [W]
Wp-s = Sensible heat gain from people [W]
X_b = Moisture content of desiccant bed [kg/kg]

Greek Letters

α = Absorptivity
β = Desiccant utilization factor
δ_M = Penetration depth for the moisture equation [m]
ϵ = Emissivity
ϵ_V = Ventilation air mixing efficiency factor
f = Script f factor for radiation
η = Effectiveness
λ = Heat of vaporization [J/kg]
ρ = Density [kg/m^3]
σ = Stefan-Boltzman Constant [$W/m^2.K^4$]
τ = Time [s]
ϕ = Relative humidity [0 to 1]

Subscripts and Superscripts

a = Air
b = Desiccant bed
des = Desiccant system air
i,j,k,l = Node or surface index
o = Outer
r = Room air
sat = Saturation state
sky = Sky
w = Water
1,2,... = State points
* = Surface condition
α = Ambient

REFERENCES

ANSI/ASME. 1985. "Measurement uncertainty: Instruments and apparatus." ANSI/ASME Standard PTC 19.1, 1985.

Barlow, R. 1982. "Analysis of the adsorption process and of desiccant cooling systems -- A pseudo-steady-state model for coupled heat and mass transfer." SERI/TR-631-1330. Solar Energy Research Institute, Golden, CO.

Collier, R.K. 1988. "Advanced desiccant materials assessment, phase II." Final Report, GRI-88/0125. Gas Research Institute, Chicago, IL.

Fairey, P., A. Kerestecioglu, and R. Vieira. 1986. "Analytical investigation of the desiccant enhanced nocturnal radiation cooling concept." FSEC-CR-152-86. Florida Solar Energy Center, Cape Canaveral.

Fairey P., R. Vieira, and A. Kerestecioglu. 1985. "Desiccant enhanced nocturnal radiation: A new passive cooling concept." Proceedings, 10th National Passive Conference, Raleigh, North Carolina. Oct 17-19.

Jurinak, J. 1982. "Open cycle solid desiccant cooling -- Component models and system simulations." Ph.D. thesis, Dept. of Mech. Eng., University of Wisconsin-Madison.

Kerestecioglu, A., Swami, M., Dabir, R., Razzaq, N., and Fairey, P. 1988. "Theoretical and computational investigation of algorithms for simultaneous heat and moisture transport in buildings." FSEC-CR-191-88. Florida Solar Energy Center, Cape Canaveral.

Kerestecioglu, A., M. Swami, and A. Kamel. 1990. "Theoretical and computational investigation of simultaneous heat and moisture transfer in buildings: Effective penetration depth theory." ASHRAE Transactions, Vol. 96, Part 1.

McClain-Cross, I.L. 1974. "A theory of combined heat and mass transfer in regenerators." Ph.D. thesis, Dept. of Mech. Eng., Monash University, Australia.

Swami., M, A. Rudd, P. Fairey, S. Patil, A. Kerestecioglu, and S. Chandra. 1989. "An assessment of the DESiccant enhanced RADiative (DESRAD) cooling concept and a description of the diurnal test facility." FSEC-CR-237-88. Florida Solar Energy Center, Cape Canaveral, FL. DOE Contract number DE-FC03-86SF16305.

TABLE 1
Zone Energy Balance Components

Term	Description	Equation
Qequ-s	Energy gains from equipment	$Ue_i\ We\text{-}s_i\ (1\text{-}Re_i)$
Qinf-s	Energy gain or loss due to infiltration	$V_i\ (II_i\ \rho_a C_p T_\alpha - EI_i\ \rho_a C_p Tr_i)$
Qlig-s	Convective energy gains from lighting	$Ul_i\ Wl_i\ fc_i$
Qmix-s	Energy added or removed by internal flows	$V_i\ (\sum_{j=1}^{noz} IM_{i,j}\rho_a C_p Tr_j - \sum_{j=1}^{noz} EM_{i,j}\rho_a C_p Tr_i)$
Qpeo-s	Convective gain from occupants	$Np_i\ Wp\text{-}s_i\ (1 - Rp_i)$
Qsup-s	Energy added or removed by supply air	$\dot{m}_i C_p\ (T_{sup,i} - Tr_i)$
Qven-s	Energy gain or loss due to ventilation	$\epsilon_V\ V_i\ (IV_i\ \rho_a C_p T_\alpha - EV_i\ \rho_a C_p Tr_i)$
Qwal-s	Energy flow between zone and interior envelope surfaces	$\sum_{k=1}^{nos} h_{Ti,k} A_{i,k}\ (T^*_{i,k} - Tr_i)$ on Γ_a

TABLE 2
Zone Moisture Balance Components

Term	Description	Equation
Qcon-l	Moisture condensation	$\sum_{k=1}^{nos} h_{Mi,k} A_{i,k}\ (Wr_i - W^*_{i,k})$
Qequ-l	Moisture gains from equipment	$Ue_i\ We\text{-}l_i/\lambda$
Qinf-l	Moisture added or removed by infiltration	$V_i\ (II_i\ \rho_a W_\alpha - EI_i\ \rho_a Wr_i)$
Qmix-l	Moisture added or removed by internal flows	$V_i\ (\sum_{j=1}^{nos} IM_{i,j}\rho_a Wr_j - \sum_{j=1}^{nos} EM_{i,j}\rho_a Wr_i)$
Qpeo-l	Moisture gain from occupants	$Np_i\ Wp\text{-}l_i/\lambda$
Qsup-l	Moisture removed by supply air	$\dot{m}_i\ (W_{sup,i} - Wr_i)$
Qven-l	Moisture added or removed by ventilation	$\epsilon_V V_i\ (IV_i \rho_a W_\alpha - EV_i \rho_a Wr_i)$
Qwal-l	Moisture adsorbed or desorbed by envelope	$\sum_{k=1}^{nos} h_{Mi,k} A_{i,k}\ (W^*_{i,k} - Wr_i)$ on Γ_a

TABLE 3
Input Parameters

Measured Parameter	Bias Limit	Precision Index	Nominal Values	Sensitivity Increment
Inlet dry-bulb, °F	0.1	0.1079	77.79	0.2
Outlet dry-bulb, °F	0.1	0.05247	84.08	0.2
Inlet dew point, °F	0.1	0.1637	67.99	0.3
Outlet dew point, °F	0.1	0.06927	59.34	0.3
Orifice dry-bulb, °F	0.2	0.06545	78.05	0.2
Orifice dew point, °F	0.3	0.2076	68.01	0.3
Orifice press, in. water	0.01	0.000926	5.208	0.01
Barometric press, Pa	102	27.36	101300	102

TABLE 4
Summary of Result Uncertainty

	w.in	w.out	air density	q.sen	q.lat	air flow	water ads.
Bias Limit	5.41E-05	4.09E-05	4.49E-04	3.55E-03	7.38E-03	4.33E-05	2.90E-06
Precision Index	8.52E-05	2.74E-05	1.61E-04	3.01E-03	1.01E-02	4.97E-06	3.96E-06
Percent Uncertainty (+/-)							
95% Coverage	1.2	0.6	0.0	4.4	4.9	0.1	4.9
99% Coverage	2.1	1.1	0.1	8.0	8.5	0.1	8.5

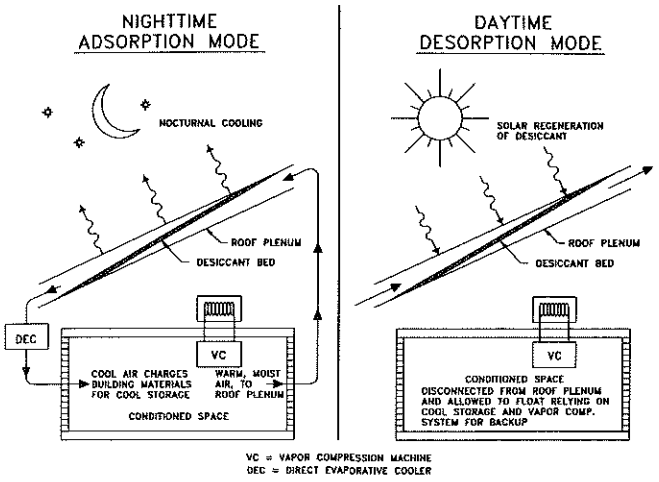

Figure 1. *Basic operating modes of the DESRAD cycle*

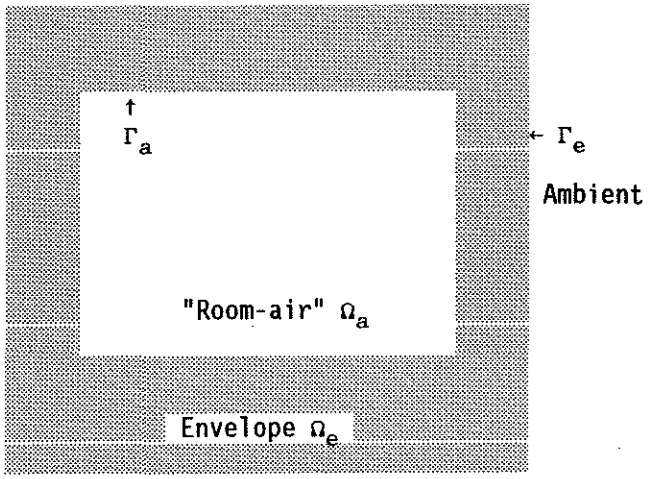

Figure 2. *Building domains and boundaries*

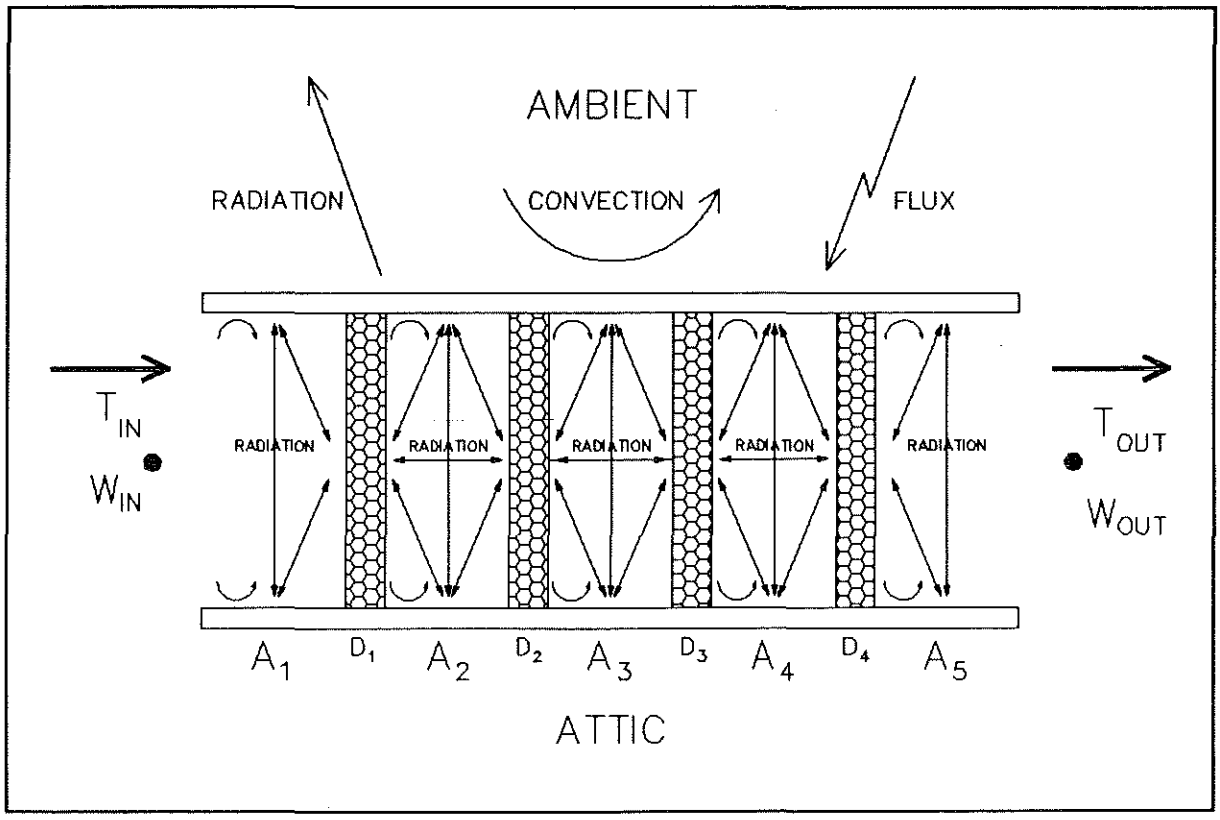

Figure 3. *Overall problem--roof desiccant system*

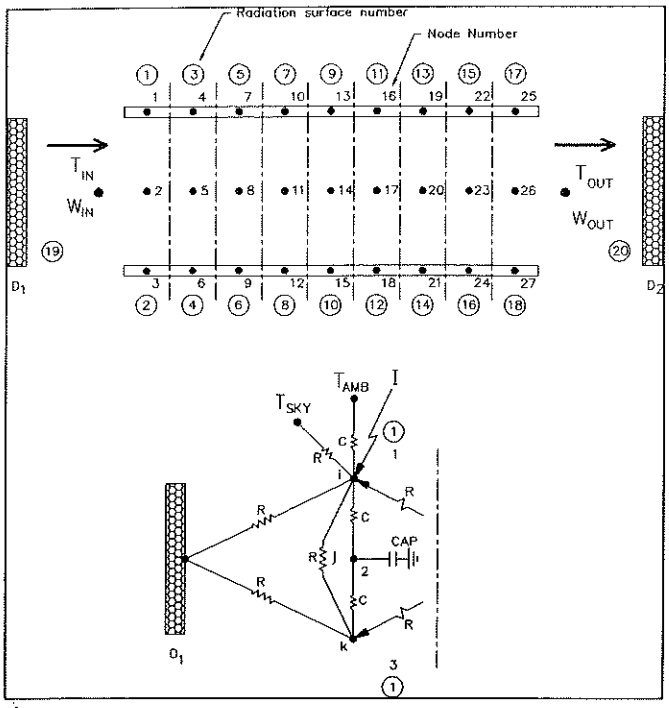

Figure 4. *Duct model*

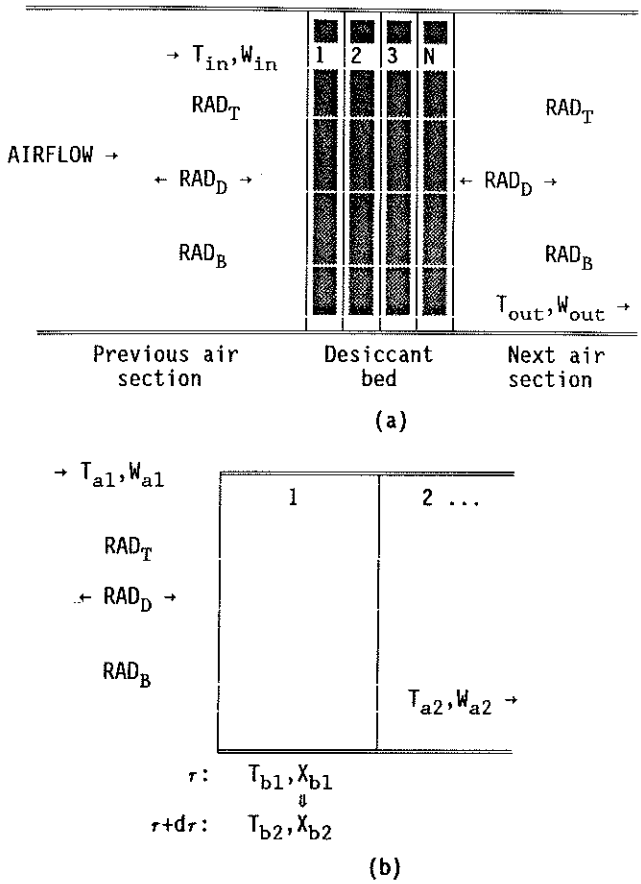

Figure 5. *(a) Desiccant bed model schematic and (b) one subsection of a desiccant bed*

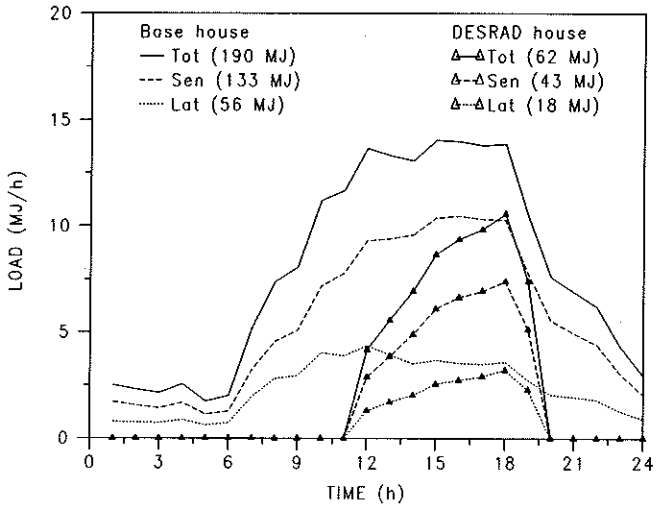

Figure 6. *Comparison of summer day cooling load requirements for base and DESRAD houses in Atlanta, GA*

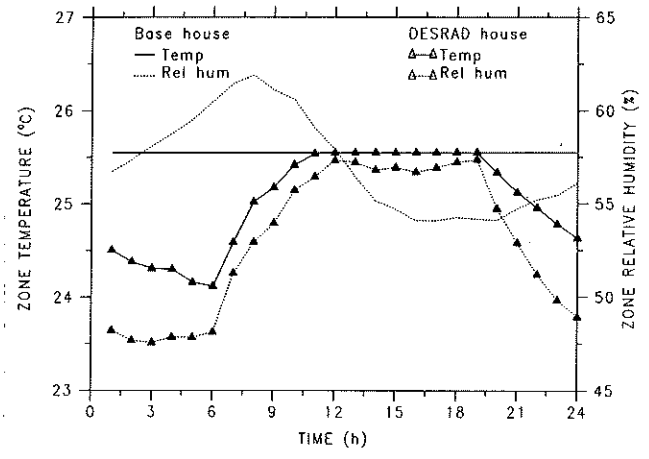

Figure 7. *Indoor conditions for base and DESRAD houses in Atlanta, GA*

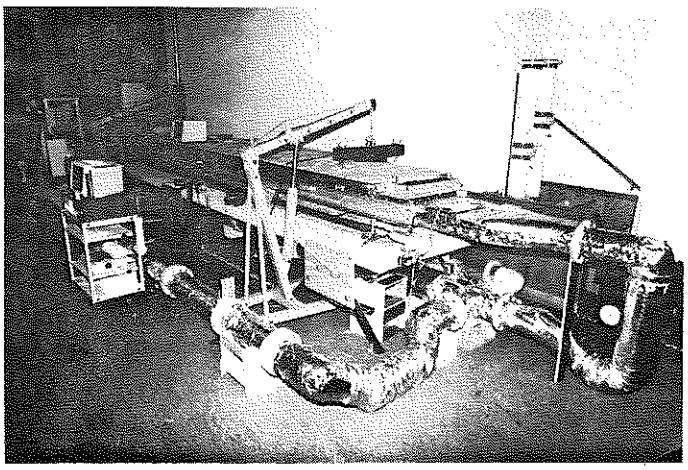

Figure 8. *Picture of the test facility*

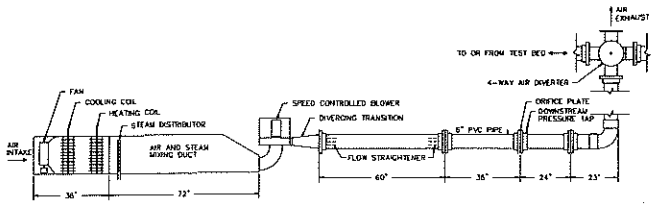

Figure 9. *Layout of the air delivery apparatus*

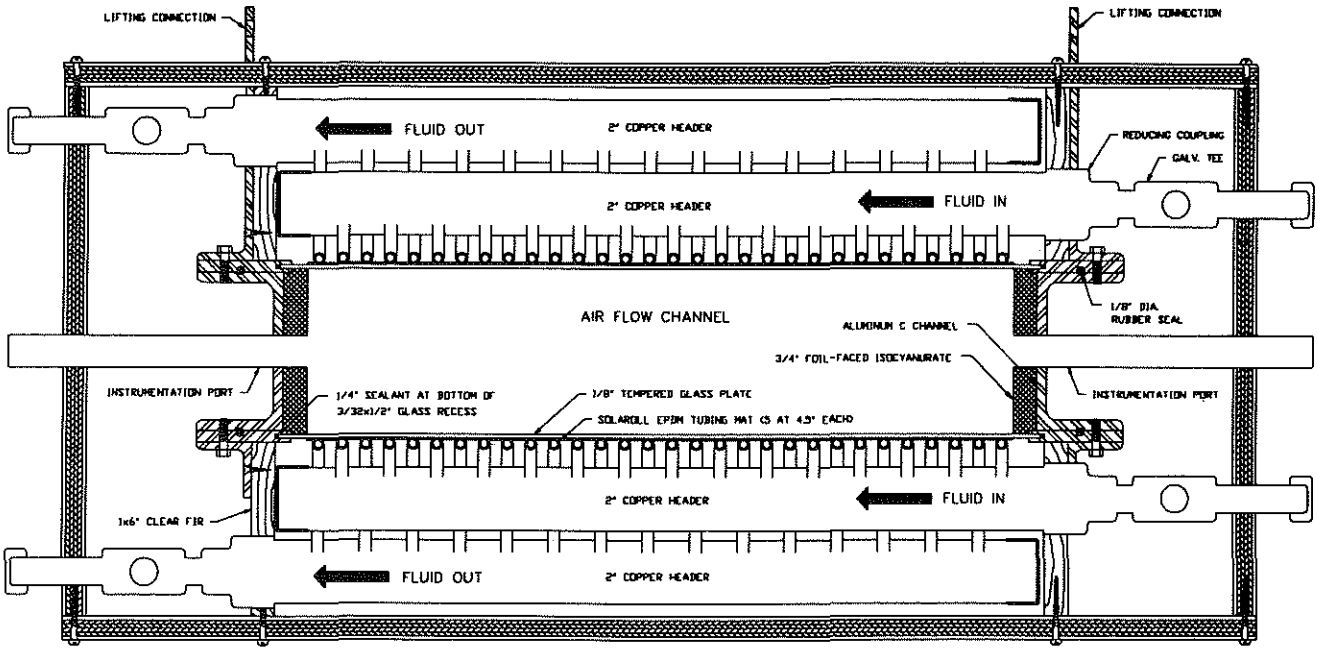

Figure 10. *Cross sectional view of the test bed*

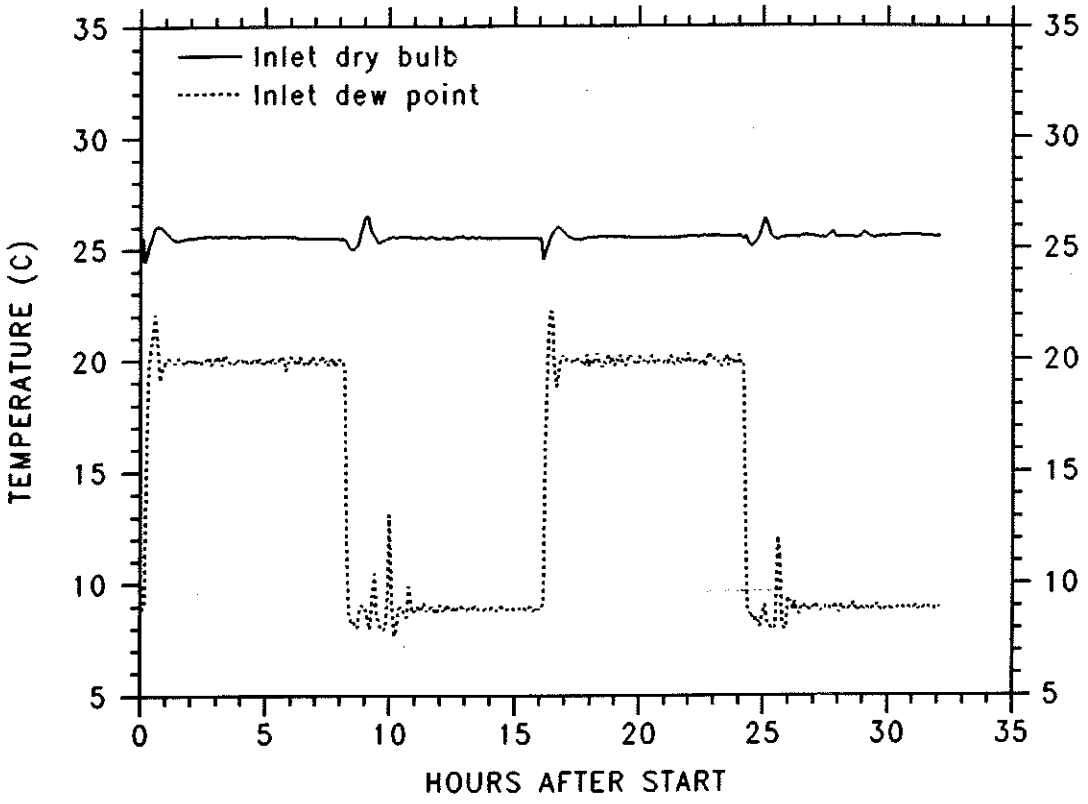

Figure 11. *Inlet air conditions for the humidity cycling test for the two-bed configuration*

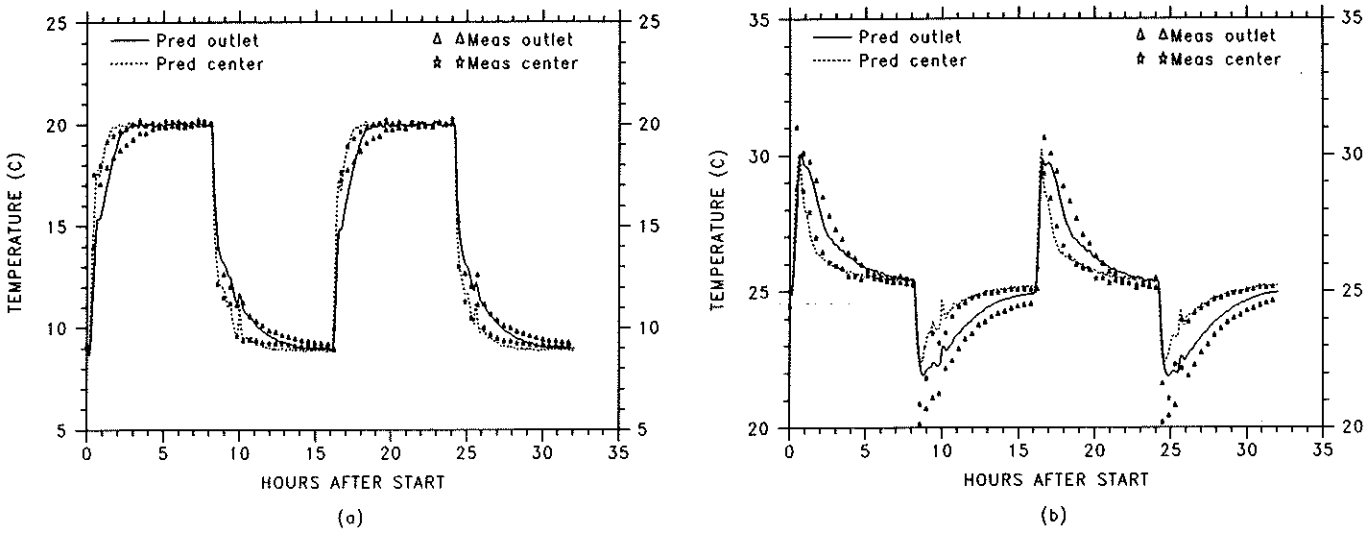

Figure 12. *Comparison of predicted and measured dew point temperatures for the two-bed configuration: (a) dewpoint temperatures; (b) dry bulb temperatures*